Single-channel recording of ligand-gated ion channels

Martin Mortensen & Trevor G Smart

Department of Pharmacology, University College London, Gower Street, London WC1E 6BT, UK. Correspondence should be addressed to T.G.S. (t.smart@ucl.ac.uk).

Published online 1 November 2007; doi:10.1038/nprot.2007.403

Electrophysiological recording of single-channel currents is the most direct method available for obtaining detailed and precise information about the kinetic behavior of ion channels. A wide variety of cell types can be used for single-channel recording, but to obtain the highest resolution of the briefest channel opening and closing events, low-noise recordings, coupled with a minimal filtering frequency, are required. Here, we present a protocol designed to help those with some electrophysiological expertise who wish to explore the properties of native and recombinant single ligand-gated ion channels. We have focused on the practical aspects of recording single GABA channels from cell-attached and outside-out patches and also introduced some of the preliminary considerations that are necessary for the analysis of single-channel data, including an introduction to single-channel analysis software.

© 2007 Nature Publishing Group http://www.nature.com/natureprotocols

INTRODUCTION

Perturbations to the resting membrane potential of a cell are often associated with alterations in its activity typified by, for example, repetitive action potential firing in neurons or by the release of hormones from glandular tissues. The underlying membrane ionic currents that change membrane potential are themselves time-averaged representations of the activity of many individual single ion channels. In essence, single channels allow a flow of current through individual pore-forming membrane proteins and by altering the amount of time for which they remain open and able to pass current; in addition, with their capacity to pass different levels of current, they fashion the electrical properties of nearly all cells.

Brief history of single-channel recording

The existence of single channels, capable of allowing charged ions to flow across the lipophilic environment of the cell membrane, was hypothesized during the late 1960s and throughout the 1970s. It had long been postulated that single-channel currents would appear as step-like changes in current as the channel opened and closed. Indeed, some of the earliest recordings of single-channel currents used lipid bilayers into which channel-forming bacterial proteins[1] or antibiotics[2] were introduced. These bilayers typically exhibited resistances in excess of 100 GΩ, thereby enabling very small currents to be resolved that exhibited discrete periods of channel opening and closure.

With regard to intact cell membranes, Katz and Miledi[3] published a seminal paper in 1972 describing a statistical analysis of fluctuations they observed in the membrane potential at the frog neuromuscular junction, which were induced by acetylcholine (ACh). This approach, which became colloquially known as 'noise analysis', predicted the existence of single ACh channels, and they used their analysis, which required several assumptions, to predict the properties of ACh-activated ion channels. The major problem that beset anyone wishing to measure single-channel currents on intact cells was the size of the background noise signal, which was sufficient to swamp the very small single-channel currents. A groundbreaking advance came when Neher and Sakmann[4] realized that electronic components possessed sufficient resolution to be able to detect single-channel currents of a few picoamperes and devised methods to reduce the level of background noise such that this no longer limited the smallest currents that could be resolved. The approach depended on electrically isolating a small patch of enzymatically cleaned cell membrane with an equally clean, heat-polished glass microelectrode. By gently pressing the pipette against the cell surface, single ion channel currents could be recorded from the extrajunctional region of the neuromuscular junction[4]. However, the seal between the electrode and the membrane was not sufficiently 'tight' compared to that achieved with lipid bilayers, with electrical leakage being evident. Nevertheless, these early recordings were able to confirm the predicted step-like changes in current that flowed through single ion channels. Neher and Sakmann[5] further noted that the durations of these currents were variable but that their amplitudes appeared to be relatively constant. At this time, some of the earliest recordings of glutamate single channels were also made from locust muscle[6]. In 1980, Sigworth and Neher[7] noted that applying slight suction to the pipette, as it rested on the cell surface, resulted in a dramatic increase in seal resistance to over 1 GΩ, and often approaching 100 GΩ. With this major breakthrough, smaller single-channel currents were resolvable, and manipulation of the membrane patch under the electrode tip became possible. Together, this made the patch clamp technique extremely versatile[8].

Patch clamp configurations

Classically, three different configurations of the patched membrane can be used for single-channel recording: cell-attached, outside-out and inside-out patches. The simplest, and least invasive, is the cell-attached configuration where the patch electrode contacts the cell membrane forming a gigaohm seal. Long-term stable recordings with low background noise can be performed in this configuration with minimal disruption to the intracellular milieu. However, the disadvantage is that one has less control over the trans-patch holding potential, as the cells' resting potential (V_m) cannot be measured, unless another electrode is used to measure this after penetrating the cell membrane. This means that the determination of the single-channel conductance (γ) from equation (1) will always be imprecise as V_m is unknown, even though

the single-channel current (i) and current reversal potential (V_{rev}) may be determined:

$$\gamma = i/(V_m - V_{rev}) \quad (1)$$

One way to try and estimate V_m is to use a concentration of KCl in the patch pipette that approximates to that found inside the cell. For example, if intracellular KCl is 140 mM and the same concentration is used in the patch pipette, then V_{rev} for potassium channel activity will be approximately 0 mV. Thus, by bringing potassium channel activity in the cell-attached patch to reversal, the patch potential (V_p) must compensate for V_m. Thus when the channels are at the reversal potential, $V_m = -V_p$, thereby providing an estimate of the membrane potential[9]. Although the success of this method rests on knowing the intracellular K^+ concentration, it is quite tolerant of some inaccuracy in $[K^+]_i$. For example, even if $[K^+]_i$ was overestimated by 10%, to 154 mM, the reversal potential and thus error in V_m would only be 2.5 mV. This increases to 11 mV for a 50% error in estimating $[K^+]_i$.

An alternative method to determine the single-channel conductance is to measure the slope conductance. This is achieved by simply changing the patch potential and noting the change in the single-channel current. Selecting a minimum of three points is sufficient to obtain an estimate of the slope conductance from $\Delta i/\Delta V_p$. Note that this estimate assumes that the slope conductance is not voltage-sensitive (reasonable for γ-aminobutyric acid-A ($GABA_A$) receptors) as V_m will still be unknown.

Identifying the channel

A further disadvantage of the cell-attached patch configuration is that the external surface of the patch can normally be exposed to only one concentration of a ligand, unless the patch electrode is internally perfused. This limits its versatility for pharmacological studies. By resorting to excised patches, some of these limitations can be overcome. For the outside-out configuration, the external surface of the patch is exposed to the external recording media. Although such patches are inherently less stable, they do offer the opportunity to repetitively expose the channels to different drugs and at various concentrations. Naturally, the binding sites for these drugs must be located on the extracellular membrane face. In the inside-out patch configuration, it is the internal face of the membrane that is exposed to the external solution. This provides access to intracellular receptor binding sites and also enables studies of intracellular signaling pathways. The excised patch is particularly useful for identifying the channel of interest. Most simply, this can be achieved by applying a selective antagonist. However, for practical purposes, it can sometimes be difficult to reverse the effects of high-affinity antagonists, so more often one might use the application of a range of agonist concentrations and monitor the changes in ion channel activity as an identifier.

It is now possible to record single-channel current activity from many cell types, that is, from mammalian species, insects, invertebrates and also plants. The recording of single-channel currents enables detailed kinetic analyses of native and recombinant ion channels, including those that have been subject to natural or intended mutations to their structure. The accumulation of kinetic data also permits the construction of plausible receptor models, which describe how many open, closed and desensitized states are necessary to account for ion channel operation as well as indicate the likely values of rate constants for the transitions of the channel from one state to another.

Noise analysis

Two alternative techniques that can be used to obtain fundamental parameters regarding ion channels are stationary and non-stationary fluctuation analysis. The former method is often used when single ion channel currents are so small as to make accurate resolution difficult. The latter technique is used for channels showing non-stationary behavior (i.e., channels underlying decaying or inactivating currents)[10,11] and when such channels are physically difficult to access with a patch electrode, for example, synaptic ion channels[12–15].

However, the information obtained from such fluctuation analyses is not as extensive as that gleaned from single-channel studies, providing only the single-channel current and often the product of the number of active channels and their open probability (P_{open}). A number of assumptions are made before using this type of analysis. For example, in one of these assumptions, the channel population is assumed to be homogeneous; otherwise, the values that are obtained from the noise analysis tend to be weighted means of different populations of channels. This can be problematic if some channel populations possess quite different single-channel currents. Another problem arises if a channel exhibits openings to different conductance states; this cannot be resolved by noise analysis, which will return a time-averaged, weighted mean conductance level. Therefore, although noise analysis can, in certain situations, offer valuable insight into ion channel operation, it is fundamentally a less powerful technique compared to single-channel recording.

Here, we provide a standard protocol for recording the activity of single $GABA_A$ receptor ion channels, in cell-attached and excised patch configurations, using suitable examples of equipment. We also explain, generically, how to perform subsequent single-channel analyses. Guidance on where to find more details regarding the theory behind single-channel kinetic behavior is also provided.

MATERIALS

REAGENTS

- Cultured hippocampal or other neurons, HEK293 cells[16] (transiently transfected with $GABA_A$ receptor cDNAs in our case), or $GABA_A$ receptor stably expressing L-tk cell lines (see REAGENT SETUP)
- Internal patch pipette solution (see REAGENT SETUP)
- External Krebs buffer (see REAGENT SETUP)
- Sylgard (see REAGENT SETUP)

EQUIPMENT

- Electrode puller (Kopf, 700D)
- Anti-vibration table (Linos Photonics, 63-500)
- Faraday cage (built in-house)
- Microscope (Inverted Nikon Eclipse TE200)
- Plexiglas recording chamber (manufactured in-house; see **Fig. 1**)
- Micromanipulator (Narishige, model: MWO-3; hydraulic) ▲ CRITICAL We recommend using a micromanipulator that can be remotely controlled so that any drift in the patch electrode can be corrected without adding vibration to the system. A hydraulic manipulator is ideal, as this has no electrical components and will not introduce any electrical noise. Manipulators relying on electrical power may require additional shielding.

© 2007 Nature Publishing Group http://www.nature.com/natureprotocols

- Patch clamp amplifier (Molecular Devices, Axopatch 200B)
- Headstage (Molecular Devices, CV203BU)
- Electrode holder ▲ CRITICAL For more stable electrode positioning and less drift, we have used an electrode holder that makes two separate O-ring contacts with the glass patch pipette (constructed at UCL, see G23 Instruments, http://www.ucl.ac.uk/g23instruments/).
- Silver chloride bath electrode (see EQUIPMENT SETUP)
- Solution application system (see EQUIPMENT SETUP)
- Low-pass Bessel filter (8-pole, 48 dB per octave)
- An oscilloscope to view filtered single-channel currents during a recording (optional)
- Data acquisition system (analog to digital converter, Molecular Devices, Digidata 1320A or 1440A)
- Computer (Dell) and software for data acquisition (Clampex) and analysis (WinEDR, Clampfit, QuB or DC programs: Scan, Ekdist, HJCfit; see Analysis programs)
- Thick-walled electrode glass capillaries (Harvard Apparatus GC150-10; 1.5 mm outer diameter × 0.86 mm internal diameter, non-filamented; see PROCEDURE)
- Optional: for long-term data storage, use either a DAT or video recorder, or alternatively, record straight to hard disk and back up on DVDs or a portable hard drive (e.g., iOmega portable drive)

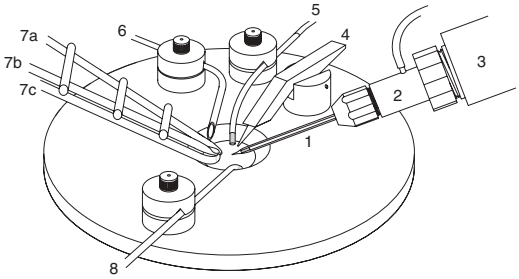

Figure 1 | Schematic of single-channel bath chamber. Surrounding the bath, the key elements of our setup are the (1) electrode, mounted on the (2) electrode holder, attached to the (3) headstage; (4) coverslip clip; (5) bath electrode assembly with the AgCl pellet mounted in a glass capillary; (6) bath solution outlet, exhaust controlled by peristaltic pump; (7) U-tube application system inlet (a), outlet (b) and auxillary tube for wash-off (c); (8) bath solution inlet gravity-fed.

REAGENT SETUP

Cells Seed cultured neurons or receptor-expressing cell lines onto poly-L-lysine-coated coverslips of 22 mm diameter. ▲ CRITICAL For the best single-channel recordings, use only very healthy cells. The health of the cell impacts on the quality of the seal formed between the cell membrane and patch pipette, which ultimately influences the critical background noise level. Cell health can be evaluated in several ways: from using cell morphology to assess cell shape, the smoothness of the cell membrane, and the integrity and position of the nucleus, to electrical assessment of the whole-cell resting membrane potential and leak current at appropriate holding potentials.

Sylgard (Dow Corning no. 184) Mix as required by adding ten parts of elastomer to one part of curing agent. Aliquots of mixed Sylgard can be stored for a few months at −20 °C or even longer at −80 °C.

Internal pipette solution: for outside-out patch recording 120 mM CsCl, 1 mM $MgCl_2$, 11 mM EGTA, 33 mM tetraethylammonium-OH, 10 mM HEPES, 1 mM $CaCl_2$ and 2 mM adenosine triphosphate (pH 7.1). This solution can also incorporate reagents to affect single-channel function, such as protein kinases, phosphatases or their inhibitors, or peptides to affect protein–protein interactions. The composition of the internal solution can vary depending on the experimental requirements. Our internal solution is designed to block background potassium channel activity and increase the internal Cl^- ion concentration such that when used with our external solution, E_{Cl} (V_{rev} in equation 1)) is close to 0 mV. This provides a large driving force ($V_m - V_{rev}$) for Cl^--mediated currents when holding patches at −60 to −90 mV. ▲ CRITICAL All solutions must be filtered. The internal solution is particularly important and should be filtered with a 0.22 µm pore diameter filter.

Internal pipette solution: for cell-attached recording Here the patch pipette solution is usually very similar to the external Krebs solution.

External recording solutions A typical external Krebs buffer contains 140 mM NaCl, 4.7 mM KCl, 1.2 mM $MgCl_2$, 2.52 mM $CaCl_2$, 11 mM glucose and 5 mM HEPES (pH 7.4). This solution can be modified to suit the experimental objectives. ▲ CRITICAL All solutions must be filtered. It is usually sufficient to filter the external solution with just standard filter paper. For most applications, ensure that the osmolarities of the internal and external solutions are approximately equivalent. Although, in principle, osmolarity can be calculated, it is better to measure it directly using a freezing-point osmometer. As expected, we find that osmolarity measured in this way is invariably slightly lower than the calculated value (internal solution osmolarity: measured 280–285 mosM, calculated 316 mosM; external solution osmolarity: measured 295–300 mosM, calculated 317 mosM). It is also important to ensure that any drug solution that is added to either the internal or external solutions does not change their pH or osmolarities. To create more stable outside-out patches, it is often advisable to ensure that the pipette solution has a slightly higher osmolarity, by approximately 10–15 mosM, compared to the external bath solution.

EQUIPMENT SETUP

Silver chloride bath electrode Solder a small Ag/AgCl pellet (5 mm long, 2 mm in diameter; Harvard Instruments) to a length of thin wire and support the assembly by inserting it into a pre-bent (∼30° angle), lightly heat-polished piece of microelectrode glass tubing. Pull the wire through the glass until the pellet sits tight up against the rim of the glass tubing. Carefully seal in position with superglue and leave to dry (see **Fig. 1**). Do not allow the glue to run all over the Ag/AgCl pellet surface.

Application system For outside-out patches, we have designed and refined a glass U-tube application system (see **Fig. 1**)[17]. The solution flows around the U-tube and is ejected over cells or patches from the apex of the tube through a small hole in the glass under vacuum control. Isolating the vacuum using solenoid switching enables rapid drug application and washout. The U-tube offers flexibility in being able to apply an unlimited succession of different drugs at different concentrations. Care should be taken in positioning the U-tube in proximity to the patch electrode, as solution vibrations and audible noise near the membrane patch can introduce electrical artifacts while recording single-channel currents. Similarly, the speed of drug/solution application onto a patch must be adjusted empirically. Placing the U-tube too near to the patch electrode and with too rapid an application can damage the electrical seal.

Earthing of the electrophysiology rig It is crucial that all the equipment in the rig have been earthed properly (avoid earth loops, that is, two different earths connected to the same piece of equipment) to minimize the background noise. It is highly recommended that initially, on setting up, only the patch clamp amplifier be connected to an oscilloscope to track any sources of electrical noise. Once these have been optimally reduced, start to connect other items of equipment one at a time, monitoring the noise level. The extent of any electrical noise can be gauged visually from the oscilloscope trace but we would recommend to use the root mean squared (r.m.s.) current setting on the patch amplifier to provide a quantitative assessment of background noise. The r.m.s. noise should, in patch mode without the electrode holder and shielding the headstage, be no higher than about 0.05 pA. The expected noise-reading with the holder connected can vary from 70 to 120 fA. Once established, sequentially turn on power-consuming equipment while studying the r.m.s. noise. This should ideally stay below 0.1 pA. Ensure that all earth leads are made from copper wire and lead back to one earth point, such as the high-quality ground on the patch clamp amplifier.

Viewing single-channel currents We recommend dividing the single-channel current signal so that an unfiltered signal can be sent straight to a disk and a filtered version can be displayed on a computer or oscilloscope screen. The latter is used to assess the state of the patch and the progress of the experiment, whereas the unfiltered signal will be used for later analysis.

Analysis programs The analysis program selected and the extent to which the experimenter wants to take the analysis is an individual choice. For a quick analysis of single-channel records that display uniform conductance levels, WinEDR, written by J. Dempster, which uses a threshold cursor to determine if the channel is in an open or shut state, is a suitable package to use and can be obtained from http://spider.science.strath.ac.uk/PhysPharm/showPage.php?

© 2007 Nature Publishing Group http://www.nature.com/natureprotocols

pageName=software_ses. An alternative commercial software suite, Clampfit (Molecular Devices), can fit different subconductance levels, but like WinEDR, its main analytical purpose is to create and fit amplitude and dwell-time distributions. For further detailed analyses, particularly where kinetic modeling of channel mechanisms and fitting of data to these models may be required, QuB created by F. Qin, L. Milescu, F. Qiong, C. Nicolai, J. Bannen, A. Auerbach, F. Sachs, A. Galick and H. Ananthakrishnan or the 'DC software' package created by D. Colquhoun (http://www.ucl.ac.uk/Pharmacology/dcpr95.html) will be needed. The idealization program, SCAN, in the DC software package, uses a time-course fitting routine that simultaneously fits all the amplitudes and durations of the single-channel currents, in contrast to the threshold cursor method, thereby increasing the attainable resolution. Both SCAN and the MIL component of QuB can fit channel subconductance levels. Note, however, that there are differences in the modeling components of QuB (MIL) and the DC software (HJCFIT), and these have been conveniently summarized on the DC software homepage (see address above).

PROCEDURE

Setup for experiment ● TIMING ~1 h

1| Prepare fresh external solution in distilled water and filter.

2| Prepare the internal solutions on the previous day and store at 4 °C. Add ATP to the internal solution only on the day of the experiment.

3| It is recommended that the osmolarities of the internal and external solutions are measured again before each experiment commences.

? TROUBLESHOOTING

4| Fabricate patch-recording electrodes. Electrodes with a small tip diameter are needed to obtain patches that contain only a few or preferably one ion channel. These electrodes will therefore naturally have a high resistance. The range of resistance for a normal single-channel electrode may vary from approximately 7 to 20 MΩ and should normally be pulled from thick-walled glass. A two-stage pull process is normally necessary to obtain patch electrodes with tip diameters of no more than 1 µm. The optimal settings to be used will vary even between electrode pullers of the same model, and these settings have to be found empirically. The first-stage pull settings should allow the glass capillary to thin over a drop of approximately 5 mm. These initial settings are usually not so critical. The more precise second-stage pull settings should create two near-identical electrodes with resistances of around 6–8 MΩ.

▲ **CRITICAL STEP** The ion channel density on the cell surface of the recording cell will be of importance when designing the optimal electrode resistance. The level of expression for cell surface receptors in heterologous expression systems can be partly controlled by diluting the cDNA concentration used for transfection. This is often achieved by co-transfecting the cell with the receptor DNA in proportion with an 'empty' vector[18]. The relative proportion will need to be determined empirically.

? TROUBLESHOOTING

5| For the lowest noise, highest resolution recordings, coat the patch electrodes with a thin layer of Sylgard. The Sylgard coat should be applied from above the shank of the electrode to near the tip opening. Most Sylgard has a tendency to run (into the tip), so keep the tip slightly up above the horizontal. We normally apply Sylgard up to 0.3–0.5 mm from the tip. The Sylgard should then be cured, for example, by drawing it through a heated coil of nichrome wire or by using a heat gun (the curing only takes a few seconds). The Sylgard coat increases the thickness of the wall near the tip of the electrode and its hydrophobic quality prevents solution from creeping up the electrode. Both these features decrease capacitance coupling to the bath, which helps to reduce the background noise level.

? TROUBLESHOOTING

6| Heat-polish the tip of the electrode under a dissecting microscope (magnification ×400) by bringing it close to a V-shaped piece of platinum/iridium (90/10%) wire, through which variable current is passed to obtain the desired tip opening/resistance (8–15 MΩ).

■ **PAUSE POINT** Electrodes can be stored in an air-tight sealed container. Electrodes left in open air and even for prolonged periods (>1 week) in a closed container will attract particulates, and this can interfere with successful patch clamp recording. Unused patch electrodes can be used another day, but it is wise to lightly repolish them (see Step 6) to remove any impurities or grease that may have got accumulated while in storage.

? TROUBLESHOOTING

7| Mount the cell coverslips/dishes in the recording bath and enable the bath solution exchange to remove as much particulate matter as possible from the cultured cell surfaces.

? TROUBLESHOOTING

Patching ● TIMING Varies from minutes to hours

8| Fill only the top 5–8 mm from the tip of the recording electrode with internal solution, and mount the pipette firmly on the headstage holder. Ensure that the AgCl-coated silver wire is submerged in the internal solution.

? TROUBLESHOOTING

© 2007 Nature Publishing Group http://www.nature.com/natureprotocols

9| To avoid debris from collecting at the tip, apply a small but constant positive pressure (about 5 mm Hg) to the pipette solution when entering the bath solution right up, until the moment when the pipette nearly touches the cell and causes a slight indentation of the membrane.
▲ **CRITICAL STEP** The pressure on the electrode (positive or negative) is usually controlled by a syringe (50 ml) or by mouth, depending on the preference of the experimenter. A simple water-based manometer can be used to measure the pressure.
? TROUBLESHOOTING

10| After inserting the electrode into the solution, apply a test voltage pulse (5–10 mV, 10–20 ms) and observe the leak current step by using an oscilloscope window opened within the acquisition software (e.g., Clampex seal test).

11| The slight indentation of the cell membrane will disappear when the positive pressure is released and then reversed to a small constant negative pressure. The seal resistance will increase, signified by a reduction in the leak current step, which will eventually disappear as the cell-attached configuration is formed.

12| After achieving at least a 10 GΩ seal and having set a suitable voltage clamp holding potential (e.g., +100 mV for cell-attached patches), single-channel activity may be observed, particularly if GABA or an appropriate agonist ligand has been included in the patch pipette solution (1–100 μM). Even if it has not been included, one may routinely see background channel activity. These channels can be of various types; in neurons not exposed to inhibitors, most of the activity will come from potassium channels.
▲ **CRITICAL STEP** To detect single-channel activity (particularly those with currents less than 5 pA), it is of utmost importance that the membrane seal is electrically tight ($>$20 GΩ is desirable) to minimize background noise.
? TROUBLESHOOTING

13| Channel activity is best seen by increasing the output gain on the amplifier ($\times$500) and changing the holding current. The high gain means that the input signal is using the full dynamic range of the amplifier to reflect the channel current profile more accurately.
▲ **CRITICAL STEP** For small single-channel currents, it is tempting to increase their amplitude by increasing the driving force ($V_m - V_{rev}$). Although this can be quite a successful approach, one should avoid excessive increments in the holding potential, as it can damage the patch and limit their lifetime.

14| Low-pass filter the current record, so that the single channels are resolved. Usually, this would mean filtering the signal at approximately 2–5 kHz.
▲ **CRITICAL STEP** To obtain an accurately sampled digital record of the analog single-channel current, the problem of aliasing (a type of distortion in the digital channel current signal caused by sampling the analog signal at too low a frequency) needs to be avoided. To obviate aliasing, the sampling rate used to record single-channel currents must always be at least 4–5 times faster than the filtering frequency (we sample our data at a minimum frequency of 20 kHz).
▲ **CRITICAL STEP** We recommend that the single-channel data are stored without or with only minimal low-pass filtering (no more than 10 kHz). This allows plenty of opportunities later on to filter the data at different rates to optimize the analyses.

15| Note that to change the holding potential of the cell-attached patch, one needs to apply a positive voltage to hyperpolarize the patch and a negative voltage to depolarize the patch.

16| If greater control over the patch potential is desired, then use the outside-out patch configuration, which is formed by first going to the whole-cell recording mode (see ref. 16–18). In the cell-attached configuration, voltage-clamp the cell near the expected resting potential and apply a train of voltage pulses (seal test).

17| Apply increased suction (negative pressure) until the cell membrane under the recording electrode breaks. This is observed on the oscilloscope as a sudden increase in the leak current step associated with a slowing of the capacity transients (owing to the increased surface membrane now in series with the recording electrode). There is no need to adjust the whole cell capacitance or employ series resistance compensation before forming the outside-out patch configuration.
? TROUBLESHOOTING

18| Slowly withdraw the electrode away from the cell until the leak current pulse starts reducing and the capacity transients become faster and sharper. As the outside-out patch is pulled from the cell, it is sometimes useful to gradually increase the speed of withdrawal of the pipette.
? TROUBLESHOOTING

19| The holding potential that is set on the amplifier will now determine the patch potential ($V_m = V_p$). This will provide an accurate measurement of single-channel current at any particular membrane potential and thus also the single-channel conductance at this V_m. Under our recording conditions for $GABA_A$ receptors, we normally voltage-clamp patches at −70 mV.

© 2007 Nature Publishing Group http://www.nature.com/natureprotocols

▲ CRITICAL STEP It is important to realize that very rarely will a patch have only one ion channel present. More often, multiple channels will be evident by 'ion channel current stacking', which can give a lower limit indication of the number of ion channels present in the patch, particularly when using a high ligand concentration and observing the current stacking when the patch is first exposed to the ligand and before desensitization attains a steady state. However, if channel activity is low (i.e., at low ligand concentrations), it is unlikely that all the ion channels in a patch will open simultaneously, so channel current stacking is unlikely to provide an indication of the total number of channels present. Similarly, if only one ion channel current opening is observed throughout a recording, the experimenter can never be quite sure that there is indeed only one channel present, as two channels may give rise to bursts of openings that do not overlap in time. This does not matter that much when the channels are of identical molecular composition and just the open times are being analyzed, but it is important when considering long shut periods.

20| If the aim of the study is to develop receptor-channel kinetic mechanisms, then it is important to explore the range of kinetic activities (or rarely, different conductance states) that can be exhibited by the single channels under study. Generally, many ligand-gated ion channels are activated following multiple ligand binding (most often two), yet some channel activity is also thought to represent singly liganded states. To try and encompass the various states of receptor ligation, single-channel recordings should incorporate activity induced by submaximal agonist concentrations to capture receptor states that are not saturated as well as including the activity of channels following their activation with saturating concentrations of agonists to ensure maximal binding of the agonist to the receptor. This is of particular importance when the studied receptor has more than one agonist-binding site, as only saturating concentrations are likely to define the activity of the fully liganded state(s) of the receptor. To achieve this range of activity, we have usually chosen agonist concentrations that are capable of inducing channel activity that is approximately 5%, 50% and 95% of maximum (e.g., EC_5, EC_{50} and EC_{95}). These concentrations are usually determined by recording whole-cell agonist-induced currents and from full agonist concentration response curves[19].
! CAUTION There are many aspects to single-channel data acquisition than can be covered in a single protocol. For further information, refer to refs. 20 and 21.
■ PAUSE POINT Data can be analyzed anytime after recording.

? TROUBLESHOOTING

Troubleshooting advice can be found in **Table 1**.

TABLE 1 | Troubleshooting table.

Step	Problem	Possible reason	Solution
Equipment setup: Earthing	Background noise in the rig	Inadequate shielding of external electrical signals	Check the integrity of your Faraday cage for holes or lack of earthing, etc.
			Add an additional earthed screen (usually a piece of copper mesh) in front of the recording chamber
		Experimenter acts as an aerial	Touch the earthed Faraday cage or attach an earth strap to the wrist
		Internal electrical noise (including 50 Hz noise)	Earth each piece of equipment (amplifier, headstage, oscilloscope, etc.) and associated metal that could act as aerials (e.g., metal stands, microscope, manipulators, etc.). This is achieved by connecting to an earth block attached to the inside of the Faraday cage
			Earth the terminal block to the ground socket on the amplifier
			Solution lines to and from the bath should be grounded via the insertion of short lengths of metal tubing
			Reduce the length of the Ag/AgCl wire in the electrode holder (only 5 mm longer than the holder can reduce the noise level to 60–70 fA)
12, 17 and 18	Patches are generally too noisy	The seal between the electrode and the membrane is insufficient or lost during patching	Practice patching technique. Aim for no less than 10 GΩ seals initially. Avoid excessive suction when breaking the seal to go to the whole-cell configuration. Ensure a smooth withdrawal from the cell when pulling an outside-out patch

© 2007 Nature Publishing Group http://www.nature.com/natureprotocols

TABLE 1 | Troubleshooting table (continued).

Step	Problem	Possible reason	Solution
5		Noise arising from dielectric coupling	Ensure the Sylgard coat on electrodes is sufficiently thick
			Keep solution depth in the bath low so that the electrode tip is only minimally submerged
8			Fill the tip of the electrode with internal solution just enough to cover the tip (2–4 mm) of the silver wire
Reagent setup: Cells		Poor membrane seals owing to fragile/ unhealthy or 'dirty' cells	Cell quality has to be improved by optimizing cell culture techniques (primary culturing, cell maintenance, transient transfections, etc.)
7			If cells have been transiently transfected by, for example, the $Ca_3(PO_4)_2$ technique, they may initially be covered by a DNA precipitate. Most of this can be quickly removed by washing with external solution using an application system
4		Poor membrane seals owing to less than optimal electrodes	Heat-and-pull settings on the electrode puller need optimization
6			Electrode tips must be cleaned by polishing to remove any debris (or Sylgard) that will compromise the electrical seal with the cell membrane
9			Keep the surface of the external solution as clean as possible, so that particles are not picked up by the electrode tip when entering the solution
	Slow noise oscillations during recording	Small vibrations in the bath solution	Ensure that the bath fluid level remains constant and stable during solution exchange
		Electrical 50 Hz noise	Please see above ('background noise in the rig')
	Fast noise oscillations during recording	Audible noise	Ensure that the lab is quiet with no high-pitched sounds
Equipment setup: Application system			Avoid audible noise and solution vibration from the bath suction outlet
		Physical vibration	Avoid or be extremely careful when touching objects sitting on top or connected to the anti-vibration table top (e.g., near the bath chamber or microscope, etc.)
			Limit traffic around the rig, ensure individuals walk lightly
Reagent setup: Cells	Losing patches quickly (from seconds to minutes)	Unstable membrane seals owing to unhealthy cells	Cell quality has to be improved by optimizing cell culture techniques. Note that some lipofection methods can leave cells with fragile membranes
Equipment setup: Application system		Fast solution flow damages the electrical seal	Lower and optimize the inlet flow rate for the applied solution
Reagent setup: Solutions; 3		Poorly adjusted osmolarities of solutions	Measure and adjust pipette and bath solution osmolarities

© 2007 Nature Publishing Group http://www.nature.com/natureprotocols

TABLE 1 | Troubleshooting table (continued).

Step	Problem	Possible reason	Solution
4	Patches contain too many channels	Receptor density is too high	Try adjusting the level of receptor expression (applicable for recombinant receptors) by lowering the concentration of cDNA used in the transfection
4 and 6			Alternatively, you can increase the resistance of your patch electrode (more intense polishing of the electrode tip may be enough) to encapsulate a smaller surface area of cell membrane with a lower number of receptors
	Patches contain too few channels	Receptor density is too low	Perform opposite to the solution given for the problem 'Patches contain too many channels'.

ANTICIPATED RESULTS

Single-channel records suitable for analysis

In essence, an analog single-channel record will present itself as a series of open and shut periods. By increasing the agonist concentration, channel activity can become increasingly transformed into bursts of activity, with each burst containing a series of individual open–shut periods. It is worth noting that the appearance of bursts or indeed clusters (see below) will be dependent upon the kinetics of individual ion channels, and thus not all channels may show this behavior, though typically many GABA channels do.

Using higher concentrations of agonist, clusters of activity are often evident. These clusters reflect long-lasting activity of single ion channels, and these are separated often by long desensitized periods. At high ligand concentrations, the cluster open probability is high and thus clusters are easy to identify. However, clusters can also appear at low agonist concentrations, but they can be very hard to identify when the cluster open probability is low. In contrast, bursts will be easier to identify at lower agonist concentrations owing to their high open probability. Such bursts of channel activity are still separated by long shut periods, and this is thought to mainly represent periods in which none of the channels in the patch have any bound ligand (unbound states). However, such long shut periods may also reflect sojourns in desensitized receptor states (**Fig. 2**).

Occasionally, during early times following activation by the agonist, particularly at higher concentrations, channel stacking can be observed giving some indication of the minimum number of channels present in the patch (**Fig. 3A**). This shows that recording is not done from a macropatch containing tens or hundreds of active channels, in which case channel stacking becomes difficult to discern. Although care is needed in interpreting the number of channels in a patch, channel stacking is usually easy to distinguish from a single channel jumping from one conductance state to another or channels exhibiting a mixture of lower and higher conductance states (**Fig. 3Ba–d**). Nevertheless, if there is some doubt about channel stacking, it is helpful, depending on the longevity of the patch, to examine the single-channel currents at low agonist concentrations where activity will be sporadic. Low concentrations should enable the main, most

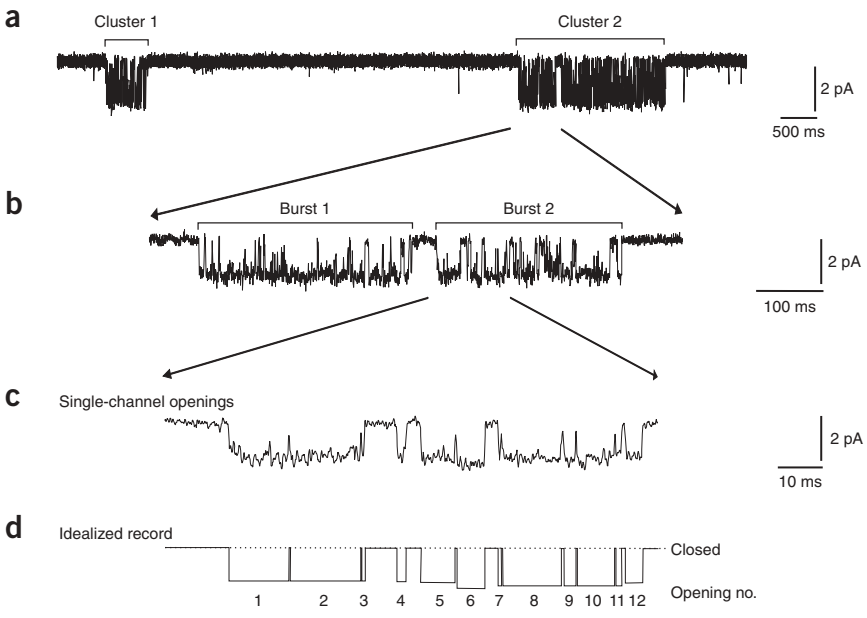

Figure 2 | Clusters, bursts and individual channel openings. Example of an outside-out patch recording of channel activity for $\alpha1\beta2\gamma2S$ $GABA_A$ receptors expressed in HEK cells in the presence of 1 mM GABA and held at −70 mV, filtered at 3 kHz and sampled at 20 kHz. Channel openings with a main amplitude of 1.9 pA can be seen as downward deflections. (**a**) Sample 9 s recording, where two distinct clusters are observed and separated by a long desensitized shut period, interrupted only by a single independent opening. A section of the second cluster is expanded in (**b**) to show how the cluster is composed of bursts of channel activity. (**c**) Further time expansion of a section of the second burst illustrates individual channel openings of different duration. (**d**) The idealized representation after having fit the original channel current with the idealization program, SCAN.

© 2007 Nature Publishing Group http://www.nature.com/natureprotocols

frequent conductance state to be clearly resolved, and if there are no inflections on the opening and shutting phases of the current, then it is unlikely to be a multiple current or channel stack. However, it could be that these low agonist concentrations elicit a lower conductance state to also appear, perhaps discretely, but if this state is not 50% of the main state (**Fig. 3Ba**), then it is also unlikely to confound the interpretation of channel stacks, as the main state cannot be a multiple. If the lower conductance is 50% of the main state (**Fig. 3Bb**), the absence of any inflections would suggest that it is not forming part of the channel stack (unless there is a complicated cooperative process for dual-channel opening). Although relatively straightforward, the interpretation becomes more complex if other conductance states appear to originate by direct transitions from the main state (**Fig. 3Bc**,**d**). Under these conditions, lowering the concentration of agonist further might enable currents without transitions and inflections to appear. If so, then these can be interpreted exactly as described above. However, if not, then the other conductance states are indeed linked by direct transitions, and although care is needed, it should still be possible to distinguish openings with subconductance states from channel stacking.

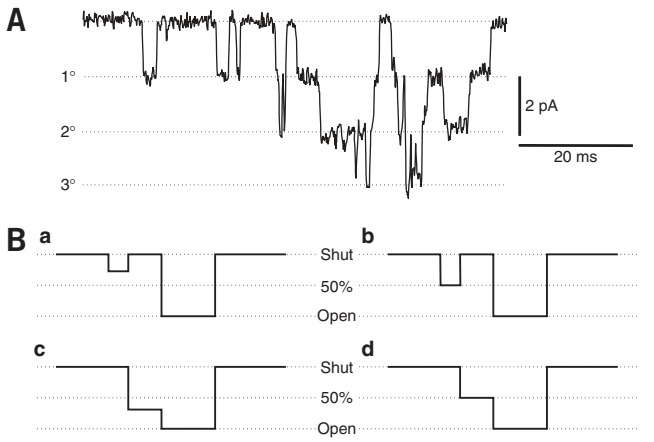

Figure 3 | Channel stacking and low versus subconductance levels. (**A**) An outside-out patch recording taken from HEK293 cells expressing $\alpha1\beta2\gamma2S$ $GABA_A$ receptors. The currents were activated by 300 μM GABA and display channel stacking (V_h: −70mV, filtered at 3 kHz and sampled at 30 kHz). The main current amplitude level for this receptor is about 1.8–1.9 pS (marked 1°), and the current stacks are multiplications of the main amplitude. Two or three channels being open in the same time window are marked as 2° or 3°, respectively. (**B**) Schematic single-channel openings displaying low conductance levels that are less than 50% (**a**) or equal to 50% of the main conductance level (**b**); or subconductance levels that differ from 50% (**c**) or are equal to 50% of the main conductance level (**d**). Low or subconductance levels that are exactly 50% of the main conductance level are probably rarely encountered, but these are shown here as possible scenarios that may need to be addressed when having to distinguish channel stacking from low or subconductance levels.

Although the presence of multiple channels in a patch is not desirable, if the frequency of these events is small (we estimate that these events should form less than 2% of all bursts), they are unlikely to confound the analysis. However, even if there is more than one active channel in a patch, long desensitized shut times can be eliminated by excising the bursts or clusters of channel activity for further analysis. As uncertainty regarding the actual number of channels in a patch is ever-present, even if no apparent channel stacking is observed, one can never interpret with complete confidence the long shut times between individual bursts or clusters.

The small currents (usually only a few picoamperes) measured in single-channel recordings naturally make the technique very sensitive to electrical artifacts. Such artifacts are usually easy to spot; however, when channel-like artifacts have conductances close to those of the receptor of interest, it can be problematic to separate them from real channel openings. If in doubt, a selective channel antagonist should be applied to evaluate if suspicious openings are artifacts or not. Seal breakdown is usually more erratic and without defined conductance levels, so these can be easily spotted, even with an untrained eye.

Idealization of the single-channel record

Usually, one of the first steps in any single-channel analysis is to idealize the current record into individual open and shut events. Precision during idealization is naturally crucial for all subsequent analysis, and will especially be important if the aim is to fit the data to a defined receptor mechanism. However, it is not always necessary to idealize the data, as the MPL component of QuB can analyze raw (non-idealized) data.

One needs to filter the data record appropriately. Some filtering of background noise is always required, but the extent of filtering should be kept to a minimum, to obtain the highest time resolution of the briefest single-channel events. When playing back the single-channel recording, the lowest possible level of filtering can be evaluated. We aim to filter at no more than 2 kHz for GABA channels and preferably between 3 and 5 kHz. If the channel data are filtered too much, brief transitions between events (shut to open or open to shut) can become distorted or lost, lowering the time resolution and affecting the dwell-time distributions.

Most single-channel programs possess one or more different automated fitting routines, which in certain programs can be improved by optimization of the parameters used in the fitting process. When automatic fitting is used, it is crucial to manually scroll through all individual single-channel events assessing the appropriateness of the fits (**Fig. 2d**), as even the best signal-to-noise recordings frequently have events that require attention (refit or deletion) because of inappropriate idealization. For example:

- Dwell times might be distorted (e.g., open or shut times are too long) because brief openings or closures are undetected or missed. This may especially occur if one is using a threshold detection measurement and the change in current level is less than 50% of the main open

© 2007 Nature Publishing Group http://www.nature.com/natureprotocols

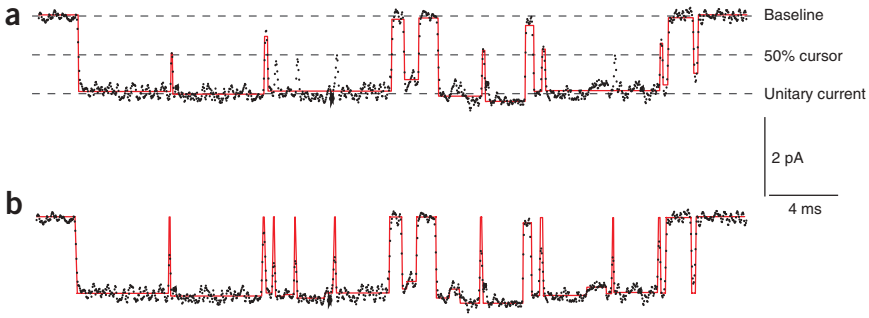

Figure 4 | Different idealization methods can lead to different results. This example of channel activity by $\alpha1\beta3\gamma2L$ $GABA_A$ receptors induced by 3 μM muscimol (outside-out patch; receptors expressed in HEK293 cells; V_h, −70 mV; filter frequency, 3 kHz; sampling frequency, 30 kHz; each sampled point is shown) has been fitted with WinEDR, which uses a 50% detection threshold cursor method in (**a**), or with SCAN, which uses a time-course fitting method in (**b**). Note how WinEDR has missed several brief shuttings, as these have not reached the 50% cursor. SCAN has the further advantage over WinEDR that it can set brief shuttings to the nearest confirmed shut level, even if this (true) level has not been detected owing to a reduction in time resolution by filtering. Two further differences between the idealization programs WinEDR and SCAN are that only SCAN will update/adjust the baseline when a well-defined shut level is observed and only SCAN can detect subconductance levels (current sublevels as part of the same opening).

state amplitude (**Fig. 4a**). To compensate for the problem of 'underdetection' of brief shuttings, one could change the threshold cursor level to lie closer to the open-channel current level; however, this will bias the detection system in favor of brief shuttings over brief openings. Similarly, one could set the threshold cursor nearer to the shut-state level. But this will then bias the detection system in favor of the detection of brief openings over brief shuttings. It is for these reasons that, to avoid bias in missed events, normally the threshold cursor would be left at 50% of the single-channel current amplitude[22]. Many of these problems can be avoided by using a time-course fitting routine[20].

- Programs using automated correction of any baseline current drift might, by over- or under-correction, cause the channel current to seemingly vary with time. This can only be corrected by resetting the baseline, where drift has occurred, following visual inspection of the data. Ensure that the single-channel currents are not altered.
- Idealized fitting may occur to a number of inappropriate conductance levels, simply because we are now following the time course of the channel current, which can exhibit some jitter (see **Fig. 4b**). It is for the analyst to decide whether such jitter in the current level represents just one or more channel conductance levels.
- The fitting routine may miss the detection of subconductance levels, or overdetect apparent transitions in current during an opening event (i.e., the channel current might just be noisy, rather than reflecting numerous conductance states). On occasions, it can be difficult to distinguish the very briefest of opening or shutting events from random noise. The best solution here is to include the events that one considers worth fitting and, at a later stage, delete those whose durations are shorter than the frequency response of the recording system.

No matter which analysis program is used, it is always important to be consistent in how you deal with individual events, thereby creating a uniform idealized event file. If you are unsure about channel current levels, there is no substitute for accruing data from more patches to assess the consistency of the single-channel current amplitudes.

How many events should be included in single-channel analyses to accurately portray the kinetic and conduction behavior of the channel? It is impossible to say exactly. The reason for this is that some events are more common than others and that some receptors show a more complex kinetic behavior than others. In our studies of $GABA_A$ receptors, we aim to include approximately 5,000–15,000 channel transition events. However, it is not always feasible to obtain that many events, especially under low agonist concentrations, where little channel activity is induced, even during quite prolonged recordings.

Stability plots

Occasionally, the kinetic behavior of an ion channel can change with time (i.e., the open probability might fall before rising again). Such non-stationarity might then confound the analysis of dwell-time distributions, particularly if all the events over the period of sampling are simply included in one histogram. To explore if changing kinetic behavior is a problem, an analysis of the overall stability of channel parameters is a common way to proceed after idealization of the single-channel currents. Even though stability plots are rarely included in publications, it is advisable to evaluate stability before performing subsequent analyses to establish the extent of any time-dependent kinetic heterogeneity in the channels.

In most single-channel analysis software, this and subsequent analysis features are usually embedded in the program. However, in D. Colquhoun's programs, software capable of analyzing stability plots, as well as amplitude histograms and subsequent dwell-time histograms requires the use of an additional program known as 'Ekdist'.

Time–stability plots can be created for many parameters, for example, single-channel current amplitude, open times, shut times and P_{open}. In principle, all these parameters can be plotted against time or event number and must, as a general rule, distribute around a stable mean throughout the whole recording. Generally, there should be no time-dependent drift in the parameter means. Naturally, there will always be a degree of scatter around the mean, but this can depend as much on the complex nature of the receptor being investigated as on the overall quality of the single-channel record. It is therefore the informed judgment of the experimenter to evaluate the quality of his/her single-channel recording before proceeding beyond this point.

© 2007 Nature Publishing Group http://www.nature.com/natureprotocols

Amplitude histograms

The current passing ability of a single open ion channel (conductance) can be analyzed by compiling single-channel current amplitude histograms. This is constructed from an event list of all the detected single-channel currents. When the channel is in a shut state, the current amplitude will be very low, near 0 pA, or will be directly assigned a value of 0 pA by the program. The open-channel currents will naturally reflect their amplitudes depending on the amplifier calibration settings. The channel current amplitudes are plotted on a linear *x* axis and their frequencies (number or percent) are represented on a linear *y* axis.

Note that all programs have default settings for binning the amplitude data to create the frequencies of occurrence for the channel currents. It is often helpful to consider alternative bin widths to reflect the data more accurately. Bin widths that are too small can overly complicate the amplitude histogram, providing a myriad of apparent current levels, whereas bin widths that are too broad have a tendency to oversimplify the histogram, obscuring the levels that should be evident. It is important that inflections on the amplitude histogram should reflect the current levels that are visually observed in the single-channel record. Mostly, we find that selecting a bin width that is approximately 0.05 times the single-channel current is often suitable for compiling an amplitude histogram. However, one should note that the fitting routine (given below for DC programs and QuB) is independent of the bin width chosen.

After construction of the amplitude histogram, all analysis programs fit Gaussian distributions (n) that define the mean single-channel (s) current (I_0), their variance (σ) and the relative areas of open and shut state populations (a), using maximum likelihood methods (**Fig. 5**):

$$n(I) = \sum_{i=1}^{n} (a_i/\sqrt{2\pi\sigma^2}) \exp(-(I_i - I_{0i})^2/2\sigma_i^2) \quad (2)$$

When applying the Gaussian probability function to the amplitude distribution, the number of Gaussians required as well as the best first estimates of their mean amplitudes, frequencies and variances must be entered into the analysis program before initiating the fitting routine. It is often advisable to start by fitting the most frequent single-channel current level by selecting its approximate mean amplitude and frequency as starting values for iterative purposes. Once a reasonable fit is achieved (altering the starting values to check the extent of the fit may have to be done), assess whether the distribution requires further Gaussians. If so, then select another peak in the distribution (often this can be done using cursors to delineate the area of the distribution to be fitted), and repeat the fitting process. Do this until all the likely components in the distribution are fitted and a range of best estimates for I_0 and σ is obtained. Finally, allow the fitting process of the entire amplitude distribution to restart by choosing the initial starting values as 'seeds' based on the single Gaussian fits. It is important to note that the Gaussian distributions are skewed inherently by the bandwidth limitations of the recording system, that is, the short duration events tend to be less reliably represented in the distribution.

Quite often, it is obvious how many amplitude/conductance states are present in the amplitude distribution, but not always. An infrequently occurring amplitude level may give rise only to a slight 'shoulder' or 'inflexion' on the amplitude histogram (**Fig. 5C**). Furthermore, two near-equally frequent but distinct channel current amplitude states may give rise only to a subtle broadening of the histogram peak. It is therefore important to evaluate not only the program's numerical output for the fit (variances, maximum likelihood, etc.), but also how visually acceptable is the summed Gaussian fit to the 'ridge' of the

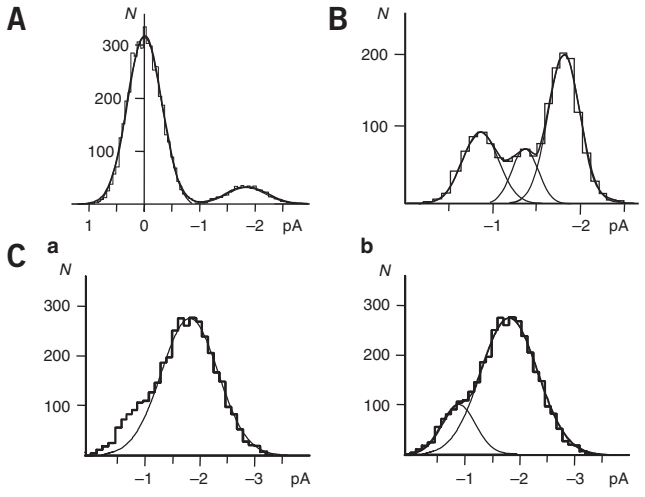

Figure 5 | Amplitude histograms fitted with Gaussian functions. Amplitude histograms can describe the number of amplitude populations, their mean current levels and their relative frequencies when fitted with Gaussian distributions. (**A**) An amplitude histogram showing both the shut state fitted with a Gaussian around zero current and a single open-channel current amplitude with a mean around 1.8 pA. The example is from an outside-out recording of $\alpha1\beta2\gamma2s$ $GABA_A$ receptor activity in the presence of 10 μM GABA. The area under the Gaussians indicates the time the receptor channel spends in the different states. The open probability (P_{open}) is a ratio between the areas of closed and open states. In this example, the P_{open} was 0.14. (**B**) In these amplitude histograms, only the open-channel current amplitudes are shown. In this example of $\alpha5\beta3\gamma3$ $GABA_A$ receptor activity, induced by 10 μM GABA, three Gaussians have been fitted, indicating the main (most frequent) amplitude level near 1.75 pA and two lower and less frequent levels near 1.3 and 0.8 pA. (**C**) Example of an amplitude histogram from neuronal $GABA_A$ receptors from hippocampal pyramidal cells in the presence of 10 μM GABA and 3 μM Zn^{2+} and fitted with one versus two Gaussians in (**a**) and (**b**), respectively. Note how an additional Gaussian is required to properly fit the slight shoulder on the left side of the histogram. All examples are from outside-out patches held at −70 mV. The current amplitude (pA) is shown on the linear *x* axis, whereas the frequency (number of observations in each bin, *N* is shown on the linear *y* axis. The thicker line following the ridge of the histogram is the sum of all fitted Gaussians.

© 2007 Nature Publishing Group http://www.nature.com/natureprotocols

histogram. A statistical assessment of the number of components required to fit the distribution can be undertaken, but generally it is better to repeat the experiment, generate new amplitude histograms and ascertain how consistent are the mean current values and the number of components required to fit the amplitude distribution from patch to patch.

Depending on the number of Gaussian components required to fit the amplitude histograms, one or more mean amplitude levels can be found for the open channel. The areas of individual components in the distribution can approximate to the relative proportion of time the channel spends at particular conductance levels. The mean conductance(s) of each open state is then calculated from the current amplitudes by considering the holding potential and reversal potentials (see equation 1)).

There are many types of amplitude histograms that can be constructed. The simplest is to take all the data points for the single-channel record (all-point-amplitude histogram) that will yield a peak around 0 pA for the shut state(s) and one or more peaks reflecting the channel currents for the open states. By comparing the areas of the Gaussian components used to fit the peaks for the open and closed states in the amplitude distribution, an approximation of the channel open probability (P_o) is occasionally derived, but we should note that between the peaks there are some points along the abscissa that are not included in the areas of the Gaussians. This leads to an overestimate of P_o (**Fig. 5A**).

An alternative point-amplitude distribution includes all individual points taken from the digitized single-channel currents (where there is one point in the histogram for every fitted amplitude). This weights equally both long and short openings. In addition, after the subtraction of the baseline currents, a comparison of the areas of the peaks allows an estimate of P_o.

However, the innate uncertainty about the number of channels in a patch means that the P_o values, however determined, will always be inaccurate. As discussed below, if a P_o value is desired, it can only be accurately determined within clusters, as these are more likely to be representations of the activity of individual channels.

Open time analysis

This is one of the two main directly observable dwell-time distributions that can be assembled from single-channel data, the other being associated with shut times. The analysis of open times is of particular interest, as this is a direct measure of the kinetic activity of the channel's open states. The distribution of all apparent open times (apparent because one cannot be totally sure that very short closures have not been missed, making the open times appear longer than is the case in reality) is usually fitted with a mixture of exponential distributions defined by

$$f(t) = \sum_{i=1}^{n} (a_i/\tau_i) \exp(-t/\tau_i) \quad (3)$$

These are characterized by a time constant, τ, and a relative area, a, where the sum of all the areas must be equal to 1. Thus, the areas are approximate measures of the number of events that fall into each component. The mean open time is then given by

$$\bar{\tau} = \sum a_i \tau_i \quad (4)$$

From the event file, an open time histogram is created (**Fig. 6a**). By plotting the open times versus their frequencies on linear axes, it is often hard to see from these histograms whether more than two exponential distributions are required for fitting the distribution. To overcome this shortcoming, dwell-time histograms are usually constructed from a distribution of the logarithm of the open times versus a square root transformation of the frequency (per unit time[23]). This transformation has a significant advantage, because the exponential now appears as a bell-shaped asymmetrical function with the peak at the value of τ. Visually, this allows relatively easy recognition of the likely mean time constants for individual exponential components that are required to fit the distribution. This makes it easier to give initial guesses for the time constants, before initiating the fitting process.

Quite often, the longer open times are thought to represent the fully bound liganded-state of a receptor, particularly as these long opening events are observed at higher frequency during exposure to high agonist concentrations.

As for the single-channel current amplitude fitting, estimates of mean open times and their areas must be entered into the program before starting the iterations. As for the fits to amplitude histograms, it is important in fitting dwell-time histograms to use the minimum number of exponentials. Some programs, like WinEDR, employ an F-test to evaluate the appropriate number of exponentials required. However, repeated experimentation on new patches will allow the correct number of exponentials that are required for the open time histogram to be deduced. If patch by patch shows significant variation in the open time distributions fits, then it is likely that too many exponentials are being used in the fitting procedure.

Shut-time analysis

Shut-time histograms are created and fitted similarly as for the open times (**Fig. 6b**). Channel shut times are useful because we can use them to separate our single-channel records into bursts or clusters of activity. The shortest shut times, which are considered to separate openings that occur during a burst event, are usually quite independent of the agonist concentration. This is because the agonist most likely stays bound to the receptor during the burst of openings. Longer shut times are

© 2007 Nature Publishing Group http://www.nature.com/natureprotocols

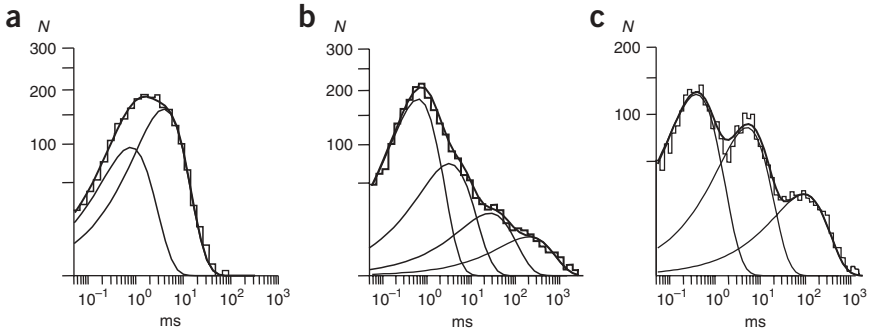

Figure 6 | Dwell-time histograms fitted with exponentials. Examples of an open time histogram (**a**), a shut-time histogram (**b**) and a burst duration histogram (**c**). All histograms are fit with an optimal number of exponentials as the dwell times are exponentially distributed. The thicker lines indicate the sums of all individual exponentials in each histogram. All three histograms are from outside-out patch recordings of the channel activity of $\alpha1\beta2\gamma2S$ $GABA_A$ receptors expressed in HEK cells in the presence of 1 mM GABA and held at −70 mV. Note that whereas the *x* axis, showing the dwell time, is logarithmic, the *y* axis, showing the frequency (number of observations in each bin, *N*), is a square root scale. In this display, it is visually easy to evaluate the histogram in terms of the optimal number of discrete populations as well as to estimate suitable means for these.

dependent on agonist concentration because they are associated with not only desensitized states, but also unliganded shut states between bursts or clusters of channel activity when the agonist has dissociated from the receptor. Of course, the number of active channels in a patch will significantly affect the numerical determination of time constants for the longer shut states, but will have no impact on time constants for shut states that occur within bursts of channel activity. If several channels are present in the patch, and opening at different times, the longest shut periods (often reflecting sojourns of the channels in either desensitized states for higher agonist concentrations or in unbound states for lower agonist concentrations) will appear shorter than they really are.

To segregate single-channel records into discrete bursts, first construct the distribution of all shut states. Those shut states that can be considered to more accurately reflect states unaffected by the number of channels in the patch (intraburst shuttings) can often be distinguished from interburst shut states by their lack of dependence on agonist concentration. Determining the shut state distributions, and their concentration dependence, from several patches exposed to different agonist concentrations is very helpful in this regard. Once this is complete, we can then attempt to define a critical shut time (t_{crit}) that lies between two components of the shut-time distribution, preferably the shortest shut times that are independent of agonist concentration (τ_{short}; inside bursts) and the longest shut times that are dependent on agonist concentration (τ_{long}; outside bursts). There are various methods to determine t_{crit} (see ref. 20), but we prefer to use the method of Colquhoun and Sakmann[24], which enables t_{crit} to be found such that equal proportions of short and long shut intervals are misclassified. This can be achieved by numerically solving the following relationship for t_{crit}

$$e^{-t_{crit}/\tau_{Short}} = 1 - e^{-t_{crit}/\tau_{Long}} \quad (5)$$

Burst analysis

It is important that the critical shut time is very carefully determined, as this value is used to define 'a burst of openings'. Thus, openings that are separated by gaps shorter than $t_{crit\ (burst)}$ are defined as belonging to a burst, whereas openings longer than or equal to $t_{crit\ (burst)}$ are considered to belong to discrete bursts. Therefore, choosing different or imprecise values for $t_{crit\ (burst)}$ will give rise to quite different selections of burst events.

Once the bursts are satisfactorily defined, there are a number of distributions that can be generated from the idealized record of single-channel open–shut events. These include, for example, distributions for burst lengths, the number of openings per burst and the total open time per burst.

Burst time duration (lengths) histograms can be generated and fit in a similar fashion as for the open- and shut-time analyses (**Fig. 6c**). For the burst lengths, we are measuring the duration from the first opening of the burst to the shutting of the last opening in the burst. The nature of this measurement is such that it will not be affected much by poor resolution of very fast openings or shuttings. In principle, the number of exponential functions required to fit the burst length distribution should be equivalent to the sum of the number of open states and those shut states that occur within a burst. However, in our practical experience, the number of exponentials required is usually much less than this. From the burst length distribution, one can calculate the mean burst duration.

The distribution of the number of openings per burst is constructed by simply counting the number of openings that appear in each burst. In this case, the histogram will be described by one or a mixture of geometric distributions[20]. The number of distributions that are required will allow some estimation of the number of kinetic transitions that are possible between channel open states and the shortest shut states that occur within the bursts.

The distribution of total open time per burst is another useful histogram to construct. As for the burst lengths, this distribution will be described by one or more exponential functions, and the number required should be the same as the number of open states that the receptor can adopt or at least provide an estimate of the minimum number of open states that exist. Knowing the open time per burst and the total burst duration, one can also derive the open probability within a burst.

© 2007 Nature Publishing Group http://www.nature.com/natureprotocols

Note that this parameter is unaffected by the number of channels in the patch, assuming that they are all of an identical molecular composition and thus expected to behave in a kinetically homogeneous fashion.

Cluster analysis

In an analogous manner to the burst analysis, one has to determine a new critical shut time that defines 'a cluster of bursts'. This time, the $t_{crit\ (cluster)}$ has to separate the shut times appearing between bursts in a cluster from those very long desensitized periods (ranging from seconds to minutes) that separate clusters. The definition of $t_{crit\ (cluster)}$ can be more difficult, as shut times on either side depend on agonist concentration. Long high-quality recordings from patches with very few channels will be required, from which the shut-time distribution ideally identifies a clear break between two long shut-time populations as the $t_{crit\ (cluster)}$.

As for the burst analysis, a number of distributions can be generated. Of particular interest is the open probability of the cluster. This parameter will be affected by agonist concentration and if a P_o–agonist concentration curve is generated, then the open probability EC_{50} for the clusters is likely to be close to that determined from an agonist concentration–response curve, after measuring whole-cell current amplitudes.

Resolution of single-channel currents

For all single-channel analyses, it is important to obtain the maximum resolution possible for the single-channel currents. Better is the resolution of a recording, more accurate the fast kinetic populations of open and shut times can be resolved. To avoid bias in the histograms for the dwell times, it is important to have a view as to what is the minimum time resolution that can be accurately recorded. To some extent, this will be a function of the dead time of the recording system, as well as the extent of filtering that is employed for the single-channel currents.

The dead time (T_d) of the system usually signifies the maximum resolution of the system, beyond which events are unlikely to be detected or only partially detected and therefore distorted. The dead time of the system can be found by applying a square wave pulse (from a signal generator) to the patch amplifier input and observing, after filtering, when the amplitude of this pulse is reduced by 50%. For a Gaussian filter, T_d can be found from

$$T_d = 0.538 T_r \tag{6}$$

where T_r is the rise time of the filter. For most single-channel work, filtering is performed with a Bessel filter whose response characteristics can be approximated by a Gaussian response. The rise time of such a filter is taken as the time that is required in moving from 10% to 90% of the output amplitude of the filter. In this case, T_r is given by

$$T_r = 0.3321/f_c \tag{7}$$

where f_c is the cutoff frequency for the filter. The limit of resolution for single-channel events can then be set based arbitrarily on a value of $1.3T_r$. Thus, for a single-channel record filtered at 2 kHz, the rise time will be (0.3321/2,000) 166 μs and the dead time will be (0.538 × 166) 89 μs. This enables us to set a maximum resolution for single-channel events, in this case of (1.3 × 166) 215 μs. However, to avoid biasing the single-channel data, it is quite normal to construct dwell-time histograms including events that are shorter than the filter rise-time, where these can be distinguished from artifacts and membrane noise (this again requires visual inspection of the data). When the histograms are compiled, then the minimum time resolution should be entered into the analysis software for the program to ignore all events of shorter duration when fitting exponential components to the distribution.

The maximum resolution of events that are included into the fitting process can also be estimated by studying the shortest (fastest) events in the shut-time histogram. If the number of events drops dramatically below a particular time duration, it most likely means that they are present but significantly underestimated, because they are not being detected owing to the fact that they are faster than the maximum resolution of the detection system. Thus, from the histogram, the minimum resolution is identified just before this steep drop. However, if this 'drop' toward faster events is more gradual, it could reflect the kinetics of the channel (i.e., these detectable fast events are simply infrequent).

Building and testing receptor-channel mechanisms

HJCfit and QuB are two leading programs for receptor modeling and analysis. The experimenter should start by exploring the simplest channel mechanisms before extending into more complicated schemes by adding additional states and/or additional connections between states.

Quite often, the number of resolved open time components in the analysis will not always equal the number of open states predicted by a model. The key output of the model is the predicted dwell-time distributions and how closely they follow the experimentally determined distributions. To avoid undue constraints on the model, it is best to first try linear kinetic schemes and delay adding cyclic models until these prove to be necessary.

© 2007 Nature Publishing Group http://www.nature.com/natureprotocols

When fitting data to a receptor-channel model, the starting estimates for the rate constants must be given. This can, at first, be difficult, but will usually become easier as the experimenter gets a better feel for appropriate values for the different parameters. Some guidance may be found from the experimental data[25–28].

Microscopic rate constants

To help the kinetic modeling, it is desirable to have realistic estimates of rate constants. For example, in the linear model, where AR* and A_2R^* are open states of the channel and R, AR and A_2R are shut states, with A_2D representing a desensitized state:

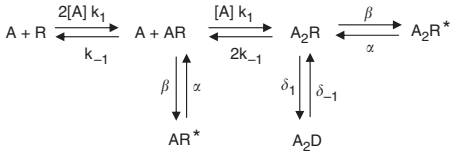

the microscopic rate constants, α, β and k_{-1}, can be calculated from the analyses of burst distributions. For example, we used estimates of the brief shut periods within a burst and the number of openings per burst to approximately determine the channel opening rate, β (refs. 19,24,25). We assume that the briefest shut periods of the channel that occur during a burst reflected the channel adopting a conformation that was typical of the A_2R state. We further assumed that the mean length of these shut periods (τ_{BS}, typified by the fast shut times, τ_{C1}, in **Fig. 6b**) will therefore be given by

$$\tau_{BS} = 1/(\beta + 2k_{-1} + \delta_1) \quad (8)$$

To simplify the analysis, we have assumed that the two agonist binding sites are equivalent, but functioning independently, and that dissociation from the diliganded state, A_2R, will be given by $2k_{-1}$. The mean number of brief shut periods (n_{BS}) per burst can then be found from

$$n_{BS} = \beta/(2k_{-1} + \delta_1) \quad (9)$$

By estimating the time constant from the brief shut periods and also the number of shut periods per burst, we can now estimate β and k_{-1} (ref. 24).

As β was estimated from the length and number of brief gaps within bursts, we would not expect desensitization to have an influence over this forward rate constant. Desensitization would invariably be accompanied by long shut periods. Furthermore, determination of β by substitution using equations (8) and (9) eliminates δ_1 in the determination of β. Finally, the desensitized periods of channel activity can be excised from the single-channel analysis by concentrating only on the kinetic properties of discrete bursts and disregarding the long shut periods.

The closure rate of the ion channel, α, was estimated by taking the reciprocal of the longest open time constant (τ_{02}), which can be determined from the distribution of all open times having been compiled after activating the receptor with the highest agonist concentration (**Fig. 6a**). A similar estimate of α can also be obtained from the reciprocal of the longest open times within bursts.

We can then use the estimates of β and α to determine the efficacy of ion channel gating from

$$E = \beta/\alpha \quad (10)$$

The calculated values for α, β and k_{-1} can now be used as starting estimates for these rate constants in suitable kinetic models (e.g., such as those compiled with HJCfit or QuB). These models will allow the underlying ion channel mechanisms as well as the consequences that mutations to the channel structure may have on ion channel kinetics to be explored. Of course, it is important to note that β cannot simply be determined from any kinetic model. The above-mentioned example is a specific case. It is important to note that this mechanism, used to describe $GABA_A$ receptor single-channel activity, is only one of a number of mechanisms that have been published over the years. See refs. 28–33 for alternatives.

In all of these models, to derive rate constant information, it is advisable to use the approaches deployed by HJCfit and QuB programs. To supplement this approach, further reading about the extensive theory behind single-channel kinetics and modeling is recommended[21].

Conclusion

For routine high-quality single-channel recording, patience is truly a virtue. Furthermore, after obtaining low-noise recordings from stable patches, the data that have been accrued can take many weeks to analyze, particularly if one is searching for a kinetic mechanism to account for the single-channel data. Although multiple solution exchanges often bring some patch instability, rapid solution exchange offers many advantages in allowing much more data to be gained from a patch. By following the protocol that has been outlined, accurate recording of low-conductance ion channel behavior should be possible. Of course, with many techniques, some optimization of the protocol may be necessary for recording particular ion channel currents. As discussed above, non-stationary noise analysis can in certain situations be useful in detecting very low conductance levels.

© 2007 Nature Publishing Group http://www.nature.com/natureprotocols

But in all other aspects of the investigation of single-channel kinetics, single-channel recording offers greater insight into the operation of ion channels.

ACKNOWLEDGMENTS We thank Marco Beato for comments on the manuscript and Guy Moss for discussion. This work was supported by MRC and the Alfred Benzon's Foundation.

Published online at http://www.natureprotocols.com
Reprints and permissions information is available online at http://npg.nature.com/reprintsandpermissions

1. Ehrenstein, G., Lecar, H. & Nossal, R. The nature of the negative resistance in bimolecular lipid membranes containing excitability-inducing material. *J. Gen. Physiol.* **55**, 119–133 (1970).
2. Hladky, S.B. & Haydon, D.A. Discreteness of conductance change in bimolecular lipid membranes in the presence of certain antibiotics. *Nature* **225**, 451–453 (1970).
3. Katz, B. & Miledi, R. The statistical nature of the acetycholine potential and its molecular components. *J. Physiol.* **224**, 665–699 (1972).
4. Neher, E. & Sakmann, B. Single-channel currents recorded from membrane of denervated frog muscle fibres. *Nature* **260**, 799–802 (1976).
5. Neher, E., Sakmann, B. & Steinbach, J.H. The extracellular patch clamp: a method for resolving currents through individual open channels in biological membranes. *Pflugers Arch.* **375**, 219–228 (1978).
6. Patlak, J.B., Gration, K.A. & Usherwood, P.N. Single glutamate-activated channels in locust muscle. *Nature* **278**, 643–645 (1979).
7. Sigworth, F.J. & Neher, E. Single Na^+ channel currents observed in cultured rat muscle cells. *Nature* **287**, 447–449 (1980).
8. Hamill, O.P., Marty, A., Neher, E., Sakmann, B. & Sigworth, F.J. Improved patch-clamp techniques for high-resolution current recording from cells and cell-free membrane patches. *Pflugers Arch.* **391**, 85–100 (1981).
9. Verheugen, J.A., Fricker, D. & Miles, R. Noninvasive measurements of the membrane potential and GABAergic action in hippocampal interneurons. *J. Neurosci.* **19**, 2546–2555 (1999).
10. Sigworth, F.J. The variance of sodium current fluctuations at the node of Ranvier. *J. Physiol.* **307**, 97–129 (1980).
11. Hocherman, S.D. & Bezanilla, F. A patch-clamp study of delayed rectifier currents in skeletal muscle of control and mdx mice. *J. Physiol.* **493**, 113–128 (1996).
12. Traynelis, S.F., Silver, R.A. & Cull-Candy, S.G. Estimated conductance of glutamate receptor channels activated during EPSCs at the cerebellar mossy fiber-granule cell synapse. *Neuron* **11**, 279–289 (1993).
13. De Koninck, Y. & Mody, I. Noise analysis of miniature IPSCs in adult rat brain slices: properties and modulation of synaptic GABAA receptor channels. *J. Neurophysiol.* **71**, 1318–1335 (1994).
14. Benke, T.A. *et al.* Mathematical modelling of non-stationary fluctuation analysis for studying channel properties of synaptic AMPA receptors. *J. Physiol.* **537**, 407–420 (2001).
15. Hartveit, E. & Veruki, M.L. Studying properties of neurotransmitter receptors by non-stationary noise analysis of spontaneous postsynaptic currents and agonist-evoked responses in outside-out patches. *Nat. Protoc.* **2**, 434–448 (2007).
16. Thomas, P. & Smart, T.G. HEK293 cell line: a vehicle for the expression of recombinant proteins. *J. Pharmacol. Toxicol. Methods* **51**, 187–200 (2005).
17. Thomas, P. & Smart, T.G. *Current Protocols in Pharmacology* (eds. Enna, S.J. *et al.*), 11.4.1–11.4.34 (John Wiley & Sons, New Jersey, 2002).
18. Groot-Kormelink, P.J., Beato, M., Finotti, C., Harvey, R.J. & Sivilotti, L.G. Achieving optimal expression for single channel recording: a plasmid ratio approach to the expression of alpha 1 glycine receptors in HEK293 cells. *J. Neurosci. Methods* **113**, 207–214 (2002).
19. Mortensen, M. *et al.* Activation of single heteromeric GABA(A) receptor ion channels by full and partial agonists. *J. Physiol.* **557**, 389–413 (2004).
20. Colquhoun, D. & Sigworth, F.J. *Single-Channel Recording* (eds. Sakmann, B. & Neher, E.) 483–587 (Plenum Press, New York, 1995).
21. Sakmann, B. & Neher, E. *Single-Channel Recording* (eds. Sakmann, B. & Neher, E.) (Plenum Press, New York, 1995).
22. Dempster, J. *Computer Analysis of Electrophysiological Signals* (Academic Press, London, 1993).
23. Sigworth, F.J. & Sine, S.M. Data transformations for improved display and fitting of single-channel dwell time histograms. *Biophys. J.* **52**, 1047–1054 (1987).
24. Colquhoun, D. & Sakmann, B. Fast events in single-channel currents activated by acetylcholine and its analogues at the frog muscle end-plate. *J. Physiol.* **369**, 501–557 (1985).
25. Hatton, C.J., Shelley, C., Brydson, M., Beeson, D. & Colquhoun, D. Properties of the human muscle nicotinic receptor, and of the slow-channel myasthenic syndrome mutant εL221F, inferred from maximum likelihood fits. *J. Physiol.* **547**, 729–760 (2003).
26. Burzomato, V., Beato, M., Groot-Kormelink, P.J., Colquhoun, D. & Sivilotti, L.G. Single-channel behavior of heteromeric α1β glycine receptors: an attempt to detect a conformational change before the channel opens. *J. Neurosci.* **24**, 10924–10940 (2004).
27. Popescu, G. & Auerbach, A. Modal gating of NMDA receptors and the shape of their synaptic response. *Nat. Neurosci.* **6**, 476–483 (2003).
28. Lema, G.M. & Auerbach, A. Modes and models of GABAA receptor gating. *J. Physiol.* **572**, 183–200 (2006).
29. Celentano, J.J. & Wong, R.K. Multiphasic desensitization of the $GABA_A$ receptor in outside-out patches. *Biophys. J.* **66**, 1039–1050 (1994).
30. MacDonald, R.L., Rogers, C.J. & Twyman, R.E. Kinetic properties of the $GABA_A$ receptor main conductance state of mouse spinal cord neurones in culture. *J. Physiol. (Lond.)* **410**, 479–499 (1989).
31. Jones, M.V. & Westbrook, G.L. Desensitized states prolong $GABA_A$ channel responses to brief agonist pulses. *Neuron* **15**, 181–191 (1995).
32. Haas, K.F. & MacDonald, R.L. $GABA_A$ receptor subunit γ2 and δ subtypes confer unique kinetic properties on recombinant $GABA_A$ receptor currents in mouse fibroblasts. *J. Physiol.* **514**, 27–45 (1999).
33. Steinbach, J.H. & Akk, G. Modulation of $GABA_A$ receptor channel gating by pentobarbital. *J. Physiol.* **537**, 715–733 (2001).

© 2007 Nature Publishing Group http://www.nature.com/natureprotocols